J Wood Sci (1999) 45:384–391

ORIGINAL ARTICLE

Daniel Guitard · Hugues Masse · Hiroyuki Yamamoto
Takashi Okuyama

Growth stress generation: a new mechanical model of the dimensional change of wood cells during maturation

Received: January 28, 1998 / Accepted: January 26, 1999

Abstract A new mechanical model was developed to introduce the maturation process of wood cells theoretically. Using mechanical and physical properties of the two components of the cell wall, namely, a matrix reinforced by oriented cellulose microfibrils, it is possible to predict the relation between the anisotropic released strains and the microfibril angle. The model used in this study is based on the unified hypothesis combining the compressive stress generated in the cell wall matrix and the tensile stress originating in the cellulose microfibril as a framework. It is simple compared to the previously derived multilayered model, but it does not strictly fulfill all conditions of static equilibrium. Nevertheless, an excellent fit with observations can be obtained through varying a limited number of parameters.

Key words Growth stresses · Wood cell maturation · Cell wall · Mechanical model · Fiber composites

Introduction

During the maturation process living cells in the differentiating xylem underneath the cambium are subject to biomechanical transformations. These transformations result in a tendency to alter cell dimensions as the cells mature. As new cells are "glued" onto the older, already existing wood material, these deformations are no longer free to occur, and maturation stresses appear in the newly formed xylem. As a consequence of the mechanical equilibrium, an increment of internal stresses is induced in the inner part of the stem. Therefore, by a cumulative process, year after year, internal residual stresses develop inside the tree trunk.[1–4]

In this paper, we present a new mechanical model describing the tendency of the wood cell to deform during the maturation process on the basis of the displacement method. The "unified hypothesis"[5–9] has been used to develop the model. This hypothesis takes into account both the "lignin swelling hypothesis" proposed by Boyd[10] and the "cellulose tension hypothesis" suggested by Bamber.[11] The mechanical models proposed in this study are then used to describe the relations between released growth strains and microfibril angles (MFAs) in the S2 layers, shown by Okuyama et al. and Yamamoto et al.[5–8]

Mechanical modeling of the maturation process based on the displacement method

Virtual unique cell model

According to Yamamoto's model, a theoretical model of maturing wood,[9] the dimensional changes of new wood tissue during maturation can be more or less represented by the behavior of a virtual unique cell originally proposed by Barber.[12] In Barber's original model, the cell is reduced to the S2 layer and can be considered as a long thick-walled circular cylinder of composite fiber-reinforced material that consists of the reinforcing framework of the cellulose microfibril (CMF) and the matrix substance of the lignin–hemicellulose compound. According to the interpretation of the reinforced-matrix hypothesis[9] (H. Yamamoto, unpublished), the CMF framework exists as a bundle and the lignin–hemicellulose matrix exists as a skeleton in the cell wall; therefore, it is thought that both the CMF bundle and the matrix skeleton occupy the same domain in the macroscopic limit.

D. Guitard · H. Masse
LEPT-ENSAM, Esplanade des arts et metiers, (Universite de Bordeaux I), 33405 Talence Cedex, France

H. Yamamoto (✉) · T. Okuyama
School of Agricultural Sciences, Nagoya University, Chikusa, Nagoya 464-8601, Japan
Tel. +81 52 789 4152; Fax +81 52 789 4150
e-mail: hiro@agr.nagoya-u.ac.jp

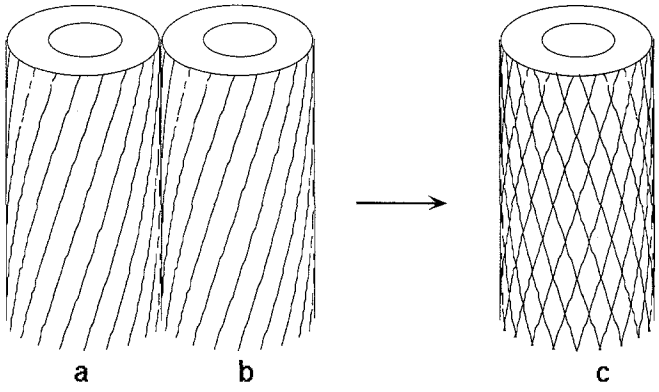

Fig. 1. Virtual unique cell model: a long, thick-walled circular cylinder of composite fiber-reinforced material. **a, b** Cell with the microfibril winding in one direction (Z-helix). **c** Virtual unique cell model with two sets of oriented microfibrils winding in opposite directions around the cell

As suggested by Barber,[12] the reinforcement in the model is obtained by two sets of oriented microfibrils winding in opposite directions around the cell (Fig. 1) with an angle of φ (i.e., the microfibril angle). Therefore one unique cell can be treated instead of a tissue of many wood cells.

Constitutive equations of the cell wall material

Mechanical presentation of the cell model

During the maturation process each one of the two phases of the material – the CMF bundle and the lignin–hemicellulose matrix – shrinks or swells. Because of the perfect bonding between the microfibrils and the matrix, internal stresses are generated; and shrinkage or swelling of each component is no longer free to occur. If a cell was able to mature alone, having no interactions with the inner tissue of the trunk, the observable dimensional change would be characterized by the strain tensor ε_{ij}, which is a tensorial unknown of the mathematical problem.

The differences between the observable strains ε_{ij} and the free maturation swelling of the matrix skeleton α_{ij}^m produce the mechanical strains $\varepsilon_{ij}^m = \varepsilon_{ij} - \alpha_{ij}^m$ developing in the matrix skeleton and supposed to be elastic. The free maturation swelling induced in the matrix skeleton α_{ij}^m comes from the mechanism of the lignin swelling hypothesis.[10] Let C_{ijkl}^m be the elastic stiffness tensor of the matrix skeleton; then, in the same way as for the thermal stress phenomenon, the associated elastic stresses become

$$\sigma_{ij}^m = C_{ijkl}^m\left(\varepsilon_{kl} - \alpha_{kl}^m\right) \tag{1}$$

In the same way, the differences between the observable strains ε_{ij} and the free maturation swelling (or shrinkage) of each one of the two sets of microfibril coatings, $\alpha^{f(+\varphi)}{}_{ij}$ and $\alpha^{f(-\varphi)}{}_{ij}$, and the associated stresses can be related by

$$\sigma_{ij}^{f(+\varphi)} = C_{ijkl}^{f(+\varphi)}\left(\varepsilon_{kl} - \alpha_{kl}^{f(+\varphi)}\right), \quad \sigma_{ij}^{f(-\varphi)} = C_{ijkl}^{f(-\varphi)}\left(\varepsilon_{kl} - \alpha_{kl}^{f(-\varphi)}\right)$$

The average stress tensor σ_{ij}^f in the laminated material of the two sets of microfibril coatings (i.e., the CMF bundle) can be given by:

$$\sigma_{ij}^f = \frac{1}{2}\left(\sigma_{ijkl}^{f(+\varphi)} + \sigma_{ij}^{f(-\varphi)}\right)$$

Therefore, we obtain:

$$\sigma_{ij}^f = C_{ijkl}^f\varepsilon_{kl} - \delta_{ij}^f \tag{2}$$

As mentioned above, both the CMF bundle and the matrix skeleton occupy the same domain in the macroscopic limit. Then, an approximation of the average stress tensor σ_{ij} in the biphasic medium (i.e., the cell wall) is given by

$$\sigma_{ij} = \sigma_{ij}^m + \sigma_{ij}^f \tag{3}$$

Elastic properties of cell wall components

Matrix skeleton The lignin–hemicellulose matrix as a skeleton is assumed to be isotropic. The components of the stiffness tensor can then be expressed using Lame's parameters λ and μ, which are directly connected to Young's modulus E^m and Poisson's ratio v^m.

The elastic constants C_{ijkl}^m of the behavior law (Eq. 1) are unchanged by rotation of the axes of reference; then nonzero terms are

$$\begin{aligned} &C_{rrrr}^m = C_{\theta\theta\theta\theta}^m = C_{zzzz}^m = \lambda + 2\mu, \\ &C_{rr\theta\theta}^m = C_{rrzz}^m = C_{\theta\theta rr}^m = C_{\theta\theta zz}^m = C_{zzrr}^m = C_{rr\theta\theta}^m = \lambda, \\ &C_{\theta z\theta z}^m = C_{zrzr}^m = C_{r\theta r\theta}^m = \mu \end{aligned} \tag{4}$$

with Lame's parameters

$$\lambda = \frac{v^m E^m}{\left(1 - 2v^m\right)\left(1 + v^m\right)} \quad \text{and} \quad \mu = \frac{E^m}{2\left(1 + v^m\right)}$$

CMF bundle The elastic properties of the CMF bundle C_{ijkl}^f, expressed along the main axes of the cell wall cylinder (r, θ, z), are more difficult to establish. The general form of elastic compliances (S_{ijkl}^{f*}), expressed along the main axes of each of the two sets of microfibril coatings, are written in Eq. (5) as functions of the elastic constants, assuming orthotropy. Then nonzero terms are

$$\begin{aligned} &S_{1111}^{f*} = 1/E_1^f, \quad S_{2222}^{f*} = 1/E_2^f, \quad S_{3333}^{f*} = 1/E_3^f, \\ &S_{1122}^{f*} = -v_{12}^f/E_2^f, \quad S_{1133}^{f*} = -v_{13}^f/E_2^f \\ &S_{2211}^{f*} = -v_{21}^f/E_1^f, \quad S_{2233}^{f*} = -v_{23}^f/E_3^f, \\ &S_{3311}^{f*} = -v_{31}^f/E_1^f, \quad S_{3322}^{f*} = -v_{32}^f/E_2^f \\ &S_{2323}^{f*} = 1/G_{23}^f, \quad S_{3131}^{f*} = 1/G_{31}^f, \quad S_{1212}^{f*} = 1/G_{12}^f \end{aligned} \tag{5}$$

It has been assumed that only normal efforts along microfibrils and shear efforts between them can be transmitted through the microfibril coating. Therefore, only E_3^f, G_{23}^f, and E_{31}^f are taken as nonzero elastic parameters. Shear moduli

are arbitrarily estimated as functions of E_3^f (i.e., $G_{23}^f = G_{31}^f = gE_3^f$, where g is a constant). When we provisionally suppose $g = 0.5$, Posisson's effects are not taken into account (i.e., $\upsilon_{12} = \upsilon_{21} = \upsilon_{23} = \upsilon_{32} = \upsilon_{31} = \upsilon_{13} = 0$). The stiffness tensor C_{ijkl}^{f*} is obtained inverting the compliance tensor S_{ijkl}^{f*} (Eq. 5). Under such restrictive but realistic conditions, the nonzero terms of C_{ijkl}^{f*} are

$$C_{3333}^{f*} = E_3^f, \quad C_{2323}^{f*} = g \cdot E_3^f, \quad C_{3131}^{f*} = g \cdot E_3^f \tag{6}$$

The components of the stiffness tensor of one of the microfibril's coating $C^{f(+\varphi)}{}_{ijkl}$ are first expressed along the main axes of the cell. They are deduced from $C^{f*}{}_{ijkl}$ as a result of the rotation of angle φ around axis 1, corresponding to the MFA.

The elastic stiffness C_{ijkl}^f of the CMF bundle, expressed along the main axes of cell, is calculated from superpositioning the two sets of microfibril coatings (which eliminates the terms with sin φ at an odd power).

$$C_{ijkl}^f = \frac{C_{ijkl}^{f(+\varphi)}}{2} + \frac{C_{ijkl}^{f(-\varphi)}}{2} \tag{7}$$

An important consequence is that the axes of cylindrical coordinates are the main axes of the CMF bundle stiffness tensor (Eq. 8), whose nonzero terms are

$$\begin{aligned} &C_{rrrr}^f, \quad C_{\theta\theta\theta\theta}^f, \quad C_{zzzz}^f, \quad C_{\theta z\theta z}^f, \quad C_{zrzr}^f, \quad C_{r\theta r\theta}^f, \quad C_{rr\theta\theta}^f, \\ &C_{\theta\theta rr}^f, \quad C_{\theta\theta zz}^f, \quad C_{zz\theta\theta}^f, \quad C_{zzrr}^f, \quad C_{rrzz}^f, \end{aligned} \tag{8}$$

The general expressions of C_{ijkl}^f are given in Appendix C, as functions of the elastic components C_{ijkl}^{f*}, g, and φ.

Free dimensional changes of cell wall components due to maturation

According to various authors,[4,7–9] the free maturation swelling of the matrix as a skeleton during the maturation process of the cell is considered an isotropic swelling strain, characterized by the parameter α (>0), so the form of the swelling $\alpha^m{}_{ij}$ ought to be a diagonal tensor:

$$diag\left(\alpha_{ij}^m\right) = \{\alpha, \alpha, \alpha\} \tag{9}$$

The free maturation swelling of each microfibril coating, assumed to be shrinkage (<0) along the microfibril direction, is characterized by a diagonal tensor, $\alpha^{f*}{}_{ij}$, when expressed with respect to the main axis of the microfibril coating.

$$diag\left(\alpha_{ij}^{f^*}\right) = \{\beta_1, \beta_1, \beta_3\} \tag{10}$$

In our particular case, the dimensional change along the longitudinal axis of the microfibril crystal (β_3) can be different from those in the transverse direction ($\beta_1 = \beta_2$).

The free maturation swelling of respective microfibril coating expressed along the main axes of the cell, $\alpha_{ij}^{f(+\varphi)}$ or $\alpha_{ij}^{f(-\varphi)}$, are then obtained from α_{ij}^{f*} through a rotation φ around axis 1.

$$\begin{aligned} &\alpha_{rr}^{f(+\varphi)} = \alpha_{rr}^{f(-\varphi)} = \beta_1, \ \alpha_{\theta\theta}^{f(+\varphi)} = \alpha_{\theta\theta}^{f(-\varphi)} \\ &\quad = \beta_1 \cos^2\varphi + \beta_3 \sin^2\varphi \\ &\alpha_{zz}^{f(+\varphi)} = \alpha_{zz}^{f(-\varphi)} = \beta_1 \sin^2\varphi + \beta_3 \cos^2\varphi \\ &\alpha_{\theta z}^{f(+\varphi)} = -\alpha_{\theta z}^{f(-\varphi)} = 2(\beta_3 - \beta_1)\cos\varphi \sin\varphi \\ &\alpha_{zr}^{f(+\varphi)} = -\alpha_{zr}^{f(-\varphi)} = \alpha_{r\theta}^{f(+\varphi)} = -\alpha_{r\theta}^{f(-\varphi)} = 0 \end{aligned} \tag{11}$$

Then, the term δ_{ij}^f in Eq. (2) is deduced using the formula

$$\delta_{ij}^f = \frac{1}{2}\left(C_{ijkl}^{f(+\varphi)}\alpha_{kl}^{f(+\varphi)} + C_{ijkl}^{f(-\varphi)}\alpha_{kl}^{f(-\varphi)}\right) \tag{12}$$

and we obtain

$$\begin{aligned} &\delta_{\theta\theta}^f = \beta_3 E_3^f \sin^2\varphi, \ \delta_{zz}^f = \beta_3 E_3^f \cos^2\varphi, \\ &\delta_{rr}^f = \delta_{\theta z}^f = \delta_{zr}^f = \delta_{r\theta}^f = 0 \end{aligned} \tag{13}$$

The term δ_{ij}^f in Eq. (2) does not depend on β_1.

Classical interpretation of the mechanical problem

Consequences of geometrical and material symmetries

The cylindrical coordinates r, θ, z are used to express the various tensor components. Because of the geometry of the cell, the homogeneity of the material properties, and assuming a spatially uniform field of shrinkage (or swelling) all over the cell wall, this mechanical problem is independent of the coordinate θ, and all derivatives versus θ are zero; $\partial / \partial \theta = 0$. Coordinates r, θ, and z correspond to the main axes of material symmetry for both stiffness and maturation swelling tensors of the matrix (C_{ijkl}^m, α_{kl}^m) and the microfibril skeleton (C_{ijkl}^f, δ_{kl}^f). As a result of the cylindrical symmetry on the field of displacements, radial displacement is only a function of r [$U_r(r)$]. As the twist effect is restricted by assumption of the axisymmetrical deformation, the tangential displacement is zero [$U_\theta(r, \theta, z) = 0$]. As the cell remains a circular cylinder after maturation, the longitudinal displacement is a linear function of z [$U_z(z) = \varepsilon_l \cdot z$], where ε_l is an unknown constant of the problem.

In such conditions, the general expression of the strain components are given in Eq. (14).

$$\begin{aligned} &\varepsilon_{rr}(r, \theta, z) = \frac{dU_r}{dr}, \quad \varepsilon_{\theta\theta}(r, \theta, z) = \frac{U_r}{r}, \\ &\varepsilon_{zz}(r, \theta, z) = \frac{dU_z}{dz} = \varepsilon_l, \\ &\gamma_{\theta z}(r, \theta, z) = \gamma_{zr}(r, \theta, z) = \gamma_{r\theta}(r, \theta, z) = 0 \end{aligned} \tag{14}$$

Introduction of Eqs. (1), (2), and (14) in Eq. (3) gives Eq. (15), which is the stress field in terms of displacements:

$$\sigma_{ij} = A_{ij}\frac{dU_r}{dr} + B_{ij}\frac{U_r}{r} - C_{ij} + D_{ij}\varepsilon_l \tag{15}$$

The details of the material tensors A_{ij}, B_{ij}, C_{ij}, and D_{ij} are given in Appendix B. In Eq. (15), the indices ij take only the values rr, $\theta\theta$, or zz because there are no shear stresses.

Formulation of the mechanical conditions

Generally speaking, σ_{ij} must satisfy the equilibrium condition (Eq. 16).

$$\sigma_{rr} - \sigma_{\theta\theta} + r\frac{d\sigma_{rr}}{dr} = 0, \quad \frac{d\sigma_{zz}}{dz} = 0 \tag{16}$$

Introduction of Eq. (15) into Eq. (16) gives a differential equation of U_r (Eq. 17).

$$\begin{aligned} rA_{rr}\frac{d^2U_r}{dr^2} + \left(A_{rr} - A_{\theta\theta} + B_{rr}\right)\frac{dU_r}{dr} - B_{\theta\theta}\frac{U_r}{r} \\ + \left(D_{rr} - D_{\theta\theta}\right)\varepsilon_{zz} + \left(C_{\theta\theta} - C_{rr}\right) = 0 \end{aligned} \tag{17}$$

We can obtain a unique solution of this equation under the boundary condition

$$\sigma_{rr}(r)\big|_{r=R_0} = \sigma_{rr}(r)\big|_{r=R_1} = 0 \tag{18}$$

where R_0 and R_1 are the inner and outer radii of the cylinder, respectively. This means there is very small turgor pressure and no transverse restriction in the fiber. By applying the solution of Eq. (17) to Eq. (15), we can determine the expressions of σ_{rr}, $\sigma_{\theta\theta}$, and σ_{zz}, although these stresses contain ε_l as an unknown parameter.

The maturation here is supposed to be free from the influence of the inner part of the trunk; therefore, no axial restriction is induced, and the average value of σ_{zz} is taken as zero. Barber[12] and Yamamoto[9] (H. Yamamoto, unpublished) then applied the following condition (integral condition) (Eq. 19) to their micromechanical analyses on the behavior of an isolated wood fiber.

$$\int_{\text{cross-section}} \sigma_{zz}\,dA = 2\pi\int_{R_0}^{R_1}\sigma_{zz}\,r\,dr = 0 \tag{19}$$

As a consequence of the above condition, we can determine the expression of the unknown parameter ε_l ($= \varepsilon_{zz}$). The components of strains ε_{rr} and $\varepsilon_{\theta\theta}$, are deduced from Eq. (14) through the solution of Eq. (17) and ε_l. The strain of the transverse dimensional change of the wood fiber model ε_t is given as $\varepsilon_{\theta\theta}|_{r=R1}$. The expressions of ε_l and ε_t are given in Appendix A.

New interpretation of the mechanical condition

Consequence of the zero stress condition (local condition)

Barber[12] and Yamamoto[9] (H. Yamamoto, unpublished) adopted the integral condition (Eq. 19) in their analysis. Equations (A1) and (A2) in Appendix A are based on the integral condition. However, in this model, the proposal is more restricting than the case of the integral condition. Directly from Eq. (15), we suppose

$$\sigma_{zz}\left(= A_{zz}\frac{dU_r}{dr} + B_{zz}\frac{U_r}{r} - C_{zz} + D_{zz}\varepsilon_l\right) = 0, \quad \text{for } {}^{\forall}r \tag{20}$$

This is a local condition, not an integral condition as adopted by Yamamoto[9] (H. Yamamoto, unpublished). The local condition sounds rather strange from the mechanical point of view. Strictly speaking, this condition is contrary to the equilibrium conditions of the stress field: It fulfills only a sufficient condition for Eq. (16) but not the necessary one. However, as described later, the local condition can explain the experimental relations between the MFA and the anisotropic maturation strain quite rationally. In that sense, we think that the local condition is a matter worthy of discussion for investigating the behavior of wood fiber cells during the maturation process.

The general solution (Eq. 21) of the differential Eq. (20) gives the radial displacement

$$U_r = cr^{-B_{zz}/A_{zz}} + \frac{C_{zz} - D_{zz}\varepsilon_l}{A_{zz} + B_{zz}}r, \quad \text{with} \quad U_z = \varepsilon_l z \tag{21}$$

where c is an integral constant. In this case, c and ε_l are unknown parameters. We can solve these unknown parameters under the boundary condition (Eq. 18), and we obtain

$$\varepsilon_l\left(= \varepsilon_{zz}\right) = \frac{C_{rr}\left(A_{zz} + B_{zz}\right) - C_{zz}\left(A_{rr} + B_{rr}\right)}{D_{rr}\left(A_{zz} + B_{zz}\right) - D_{zz}\left(A_{rr} + B_{rr}\right)}, \quad c = 0 \tag{22}$$

The components of strains ε_{rr}, $\varepsilon_{\theta\theta}$, are deduced from Eqs. (4) through (21) and (22):

$$\begin{aligned} \varepsilon_{rr} = \varepsilon_{\theta\theta} = \frac{C_{zz} - D_{zz}\varepsilon_l}{A_{zz} + B_{zz}} = \frac{1}{A_{zz} + B_{zz}} \\ \times\left(C_{zz} - D_{zz}\frac{C_{rr}\left(A_{zz} + B_{zz}\right) - C_{zz}\left(A_{rr} + B_{rr}\right)}{D_{rr}\left(A_{zz} + B_{zz}\right) - D_{zz}\left(A_{rr} + B_{rr}\right)}\right) \end{aligned} \tag{23}$$

These are equal to the strain of the transverse dimensional change of the wood fiber model, ε_t. It must be noted that the solution obtained from the local condition (Eq. 20) does not depend on values of the inner R_0 and outer R_1 cell radius. This is a direct consequence of the hypothesis in Eq. (20) (i.e., the local condition).

Assumption on the maturation swelling of the CMF bundle (averaged maturation swelling condition)

Equation (12) gives the values of δ_{ij}^f in Eq. (2). We propose the following formula to calculate them, instead of Eq. (12):

$$\delta_{ij}^f = C_{ijkl}^f\alpha_{kl}^f \tag{24}$$

where

$$\alpha_{ij}^f = \frac{\alpha_{ij}^{f(+\varphi)}}{2} + \frac{\alpha_{ij}^{f(-\varphi)}}{2} \tag{25}$$

Then Eq. (2) can be expressed in the same form as for the matrix skeleton:

$$\sigma_{ij}^f = C_{ijkl}^f\left(\varepsilon_{kl} - \alpha_{kl}^f\right)$$

The result is diagonal when expressed along the main axes of the cell:

$$diag\left(\alpha_{ij}^{f}\right) = \left\{\beta_1,\ \beta_1\cos^2\varphi + \beta_3\sin^2\varphi,\ \beta_3\cos^2\varphi + \beta_1\sin^2\varphi\right\} \quad (26)$$

On the basis of the new mechanical interpretation, that is, a combination of the local condition and the averaged maturation swelling condition, we calculated the behavior of the wood fiber model during the maturation process.

Results and discussion

Comparison to existing models

The relations between φ and ε_l, ε_t were calculated using the models proposed in this study. The results are displayed in Figs. 2 and 3. The values given by Yamamoto[9] were applied in the simulations as the parameters other than β_1, β_3, and α. The volume ratio of the cellulose crystal and the matrix substance was supposed to be 40:60. The most fitting values of β_1, β_3, and α were sought to predict the experimental tendency by the trial and error method. The description given by "the unified hypothesis" with a multilayered cell wall is shown in Fig. 4 and compared to the experimental results.

Figure 3 shows the calculated result of the model based on the integral condition, that is, Eq. (A1) and (A2). In this case, the parameters displayed in Table 1 were used, and ρ $(=R_1/R_0) = 1.5$ was assumed for the calculation. This model can explain the dependence of the transverse growth strain on φ when the value of g is assumed to be 0. However, the calculated longitudinal growth strain, which is more important for practical purposes, deviates extraordinarily from the experimental one except in the region of MFA smaller than 10 degrees. On the contrary, in the multilayered cell model reported by Yamamoto,[9] the calculated longitudinal growth strain is quantitatively consistent with the experi-

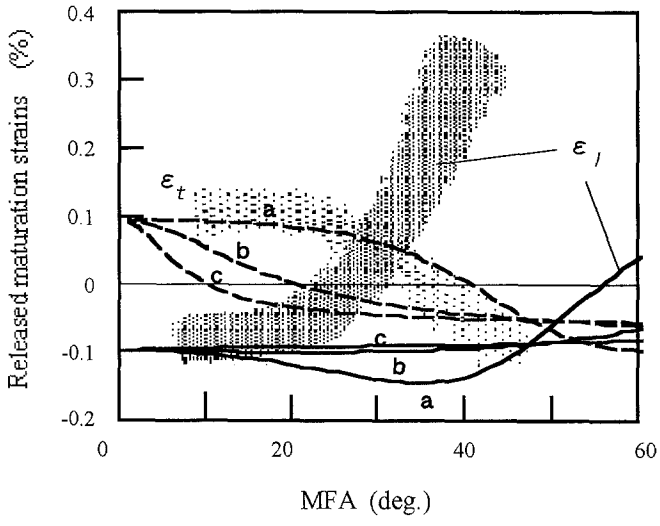

Fig. 3. Calculated released maturation strains (ε_l, ε_t) and microfibril angle (MFA) derived from the integral condition. The most fitting parameters are used (Table 1). The values of g are as follows: *a*, 0; *b*, 0.2%; *c*, 0.5%

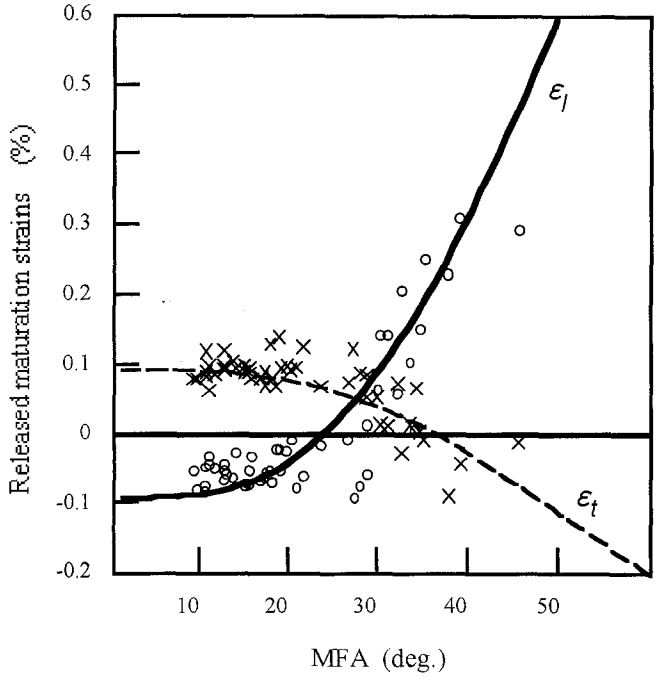

Fig. 2. Calculated released maturation strains (ε_l, ε_t) and microfibril angle (*MFA*) derived from the local condition. The most fitting parameters are used (Table 1). Dots are experimental results of two sugi trees

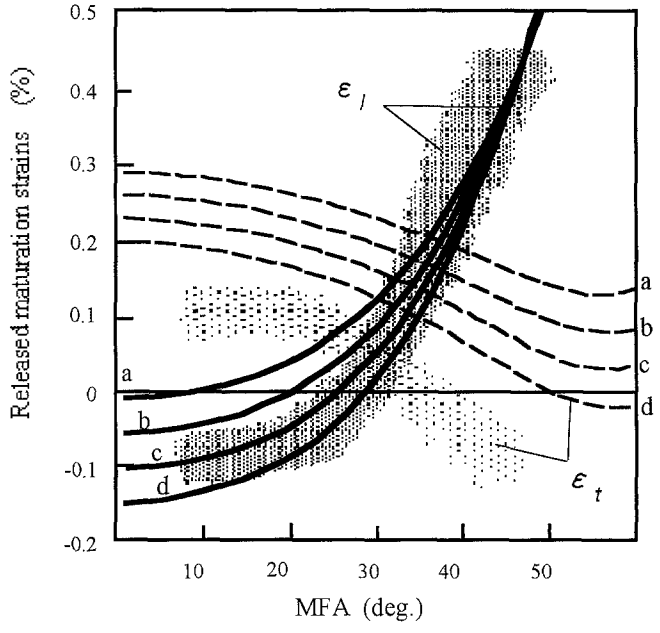

Fig. 4. Calculated released maturation strains (ε_l, ε_t) and microfibril angle (MFA) derived from Yamamoto's multilayered model (unified hypothesis model). Parameters used for the calculation are displayed in Table 1 (isotropic shrinkage). Shaded zones are the experimental tendencies of two sugi trees

Table 1. Micromechanical parameters of the matrix and microfibrils

Microfibril shrinkage	E^m (GPa)	ν^m	α (%)	E^f (GPa)	β_1 (%)	β_3 (%)
Isotropic shrinkage						
Test a	1.2	0.3	0.5	40	[a]	−0.05
Test b	1.2	0.3	0.5	40	[a]	−0.10
Test c	1.2	0.3	0.5	40	[a]	−0.15
Test d	1.2	0.3	0.5	40	[a]	−0.20
Best fit for Eqs. (A1) and (A2)	1.2	0.3	0.05	40	[a]	−0.10
Best fit for Eqs. (22) and (23)	1.2	0.3	0.05	40	+0.9	−0.10

[a] β_1 has no effect on the behavior of the cell model

mental one over a wide range of MFA, although, the multilayered model tends to overestimate the value of the transverse growth strain.

In the case of the simulation made using Eqs. (22) and (23), based on the new mechanical interpretation, not only the longitudinal growth strain but also the transverse one can be predicted quantitatively as displayed in Fig. 2 by using the parameters shown in Table 1. In this simulation, we provisionally assumed $g = 0.5$. Also in this simulation the critical MFA where the longitudinal growth strain switches from contraction to expansion is 20–30 degrees, which is consistent with the experimental MFA. Thus, it has not been necessary to use a multilayered cell wall (e.g., the model reported by Yamamoto et al.[8,9]) to obtain the critical MFA.

As we have seen, we can quantitatively predict the relation between anisotropic growth strain and microfibril angle by assuming the new mechanical interpretation. Therefore, it is believed there is some meaning in the new mechanical interpretation from the viewpoint of cell wall mechanics.

Significance of the parameter β_1

The model based on the new mechanical interpretation is advantageous for explaining the relations between anisotropic growth strains and the MFA. This advantage is derived not only from assuming the local condition and the averaged maturation swelling condition but also from introducing transverse maturation swelling of the cellulose microfibril skeleton β_1.

Figure 5 represents the effects of β_1 on the generation of the anisotropic growth strains of the model based on the new mechanical interpretation. As the value of β_1 becomes larger, the curves of ε_l and ε_t tend to shift upward and downward, respectively, from *a* to *d* in Fig. 5. In the case of $\beta_1 = 0$ (*a* in Fig. 5) it is almost impossible to explain the longitudinal compressive stress generation in the compression wood region with a large MFA. In such cases it is difficult to simulate the experimental tendency by searching fitting values of β_3 and α. Therefore, it is thought that introduction of the parameter β_1 is indispensable for elucidating the origin of the anisotropic growth stress.

It is natural to think that β_1 is concerned with swelling of the matrix regions inside the aggregation of the cellulose microfibrils caused by deposition of the matrix substance.

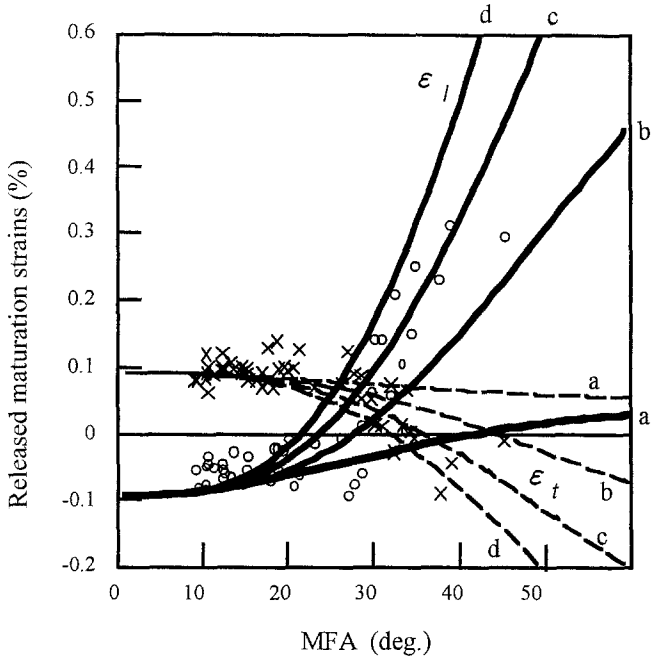

Fig. 5. Calculated released maturation strains (ε_t, ε_l) and microfibril angle (MFA) derived from the local condition, in the cases supposing various values of β_1. The most fitting parameters other than β_1 are displayed in Table 1 (best fit for Eqs. 22 and 23). Values of β_1: *a*, 0%; *b*, 0.8%; *c*, 1.6%; *d*, 2.4%

Then, it can be presumed that not only parameter α but also β_1 are induced by maturation of the matrix substance.[10] On the other hand, it is thought that β_3 is induced in the cellulose microfibril crystal by the mechanism of the cellulose tension hypothesis.[11] From the micromechanical point of view, the origin of β_3 is independent of α and β_1 generation.

Moreover, it is thought that the existence of a nonzero shear stiffness in each microfibril coating is indispensable for improving the previous models (e.g., done by Yamamoto et al.[7–9] Most previous models were developed on the basis of Barber's model,[12] in which the microfibril framework has no shear stiffness. According to Barber's conclusion "the shear forces across the plane are opposite in the two sets and canceled." On the contrary, the existence of a nonzero shear stiffness in each microfibril coating (i.e., $C^{f*}_{2323} = C^{f*}_{3131} = gE^f_3$) gives nonzero shear moduli C^f_{zrzr} and $C^f_{r\theta r\theta}$ to the stiffness tensor of the CMF bundle in the new model, as shown in Appendix C.

Conclusion

The new mechanical model, presented here, differs from previous models on three particular points: (1) The elastic behavior of the cellulose microfibrils bundle takes into account the possibility of transmiting shear efforts between fibers; then the elastic shear modulus is nonzero. (2) The most fitting conditions governing longitudinal efforts along the cell are the local condition and the averaged maturation swelling condition. The averaged values of the stress component σ_{zz} is zero on every elementary volume, instead of an integral condition on the overall cross section of the cell in other models. (3) The new model taken into account the anisotropy of the elastic properties and the dimensional changes for both the matrix skeleton and the microfibril bundle.

The model based on the new mechanical interpretation has three main advantages: (1) The predicted values of the longitudinal and transverse released strains are obtained by the explicit functions of the material properties of each component of the cell wall and the microfibril orientation. These functions are independent of the inner and outer radius of the cell cross section. (2) Under Yamamoto's material parameters,[8,9] the critical MFA is obtained at 20–30 degrees with a simple model. It is no longer necessary to introduce a multilayered model to get this result. (3) To obtain a perfect fit between experimental results and predicted values, it is necessary to consider an anisotropic dimensional change of the microfibrils. The new model suggests that the most important dimensional changes are located in the microfibril bundle, which shrinks along the fibrils and swells transversally. The swelling of the matrix skeleton is of less importance. The new interpretation, presented here, may sound strange from a mechanical viewpoint, but it offers several important speculations to experimental research on the mechanism of the unified hypothesis.[7–9]

Acknowledgments This research was carried out as a joint project under the support of the JSPS (Japan Society for the Promotion of Science) fellowship for scientific research in Japan.

References

1. Kubler H (1987) Growth stresses in trees and related wood properties. For Prod Abstr 10:61–118
2. Archer RR, Byrness FE (1974) On the distribution of tree growth stresses. I. An anisotropic plane strain theory. Wood Sci Technol 8:184–196
3. Okuyama T, Kikata Y (1975) The residual stresses in wood logs due to growth stresses. Mokuzai Gakkaishi 21:335–341
4. Fournier M, Bordonne PA, Guitard D, Okuyama T (1990) Growth-stress pattern in tree stems: a model assuming evolution with the tree age of maturation strain. Wood Sci Technol 24:131–142
5. Okuyama T, Kawai A, Kikata Y, Yamamoto H (1986) The growth stresses in reaction wood. In: Proceedings of the XVIII IUFRO World Congress, Yugoslavia, pp 249–260
6. Okuyama T (1993) Growth stresses in trees. Mokuzai Gakkaishi 39:747–756
7. Yamamoto H, Okuyama T (1988) Analysis of the generation process of growth stresses in cell walls. Mokuzai Gakkaishi 34:788–793
8. Yamamoto H, Okuyama T, Yoshida M (1995) Generation process of growth stresses in cell walls. VI. Analysis of the growth stress generation by using a cell model having three layers (S1, S2, and I + P). Mokuzai Gakkaishi 41:1–8
9. Yamamoto H (1998) Generation mechanism of growth stresses in wood cell walls: roles of lignin deposition and cellulose microfibril during cell wall maturation. Wood Sci Technol 32:171–182
10. Boyd JD (1972) Tree growth stresses. V. Evidence of an origin in differentiation and lignification. Wood Sci Technol 6:251–262
11. Bamber RK (1978) The origin of growth stresses. Contributed paper to the IUFRO conference, Philippines, pp 1–7
12. Barber NF (1969) A theoretical model of shrinking wood. Holzforschung 22:97–103

Appendix A: strains of the dimensional changes of the wood fiber model deduced by the integral condition (Eq. 19)

The longitudinal strain, ε_l, becomes

$$\varepsilon_l(=\varepsilon_{zz}) = -\frac{\bar{I}}{\bar{H}} \tag{A1}$$

$\bar{I}$ and $\bar{H}$ are composed of various variables:

$$\begin{aligned}\bar{H} = {} & \frac{N_1(A_{zz}k + B_{zz})}{k+1}\left(\rho^{k+1} - 1\right) \\ & + \frac{N_2(B_{zz} - A_{zz}k)}{1-k}\left(\rho^{-k+1} - 1\right) \\ & + \left\{\frac{A_{zz} + B_{zz}}{2(A_{rr} - B_{\theta\theta})}(D_{\theta\theta} - D_{rr}) + \frac{1}{2}D_{zz}\right\}\left(\rho^2 - 1\right)\end{aligned}$$

$$\begin{aligned}\bar{I} = {} & \frac{P_1(A_{zz}k + B_{zz})}{k+1}\left(\rho^{k+1} - 1\right) \\ & + \frac{P_2(B_{zz} - A_{zz}k)}{1-k}\left(\rho^{-k+1} - 1\right) \\ & + \left\{\frac{A_{zz} + B_{zz}}{2(A_{rr} - B_{\theta\theta})}(C_{rr} - C_{\theta\theta}) - \frac{1}{2}C_{zz}\right\}\left(\rho^2 - 1\right)\end{aligned}$$

where

$$\rho = \frac{R_1}{R_0}, \quad k = \sqrt{B_{\theta\theta}/A_{rr}}, \quad N_1 = -\frac{L}{A_{rr}k + B_{rr}}\left(\frac{\rho^{k+1} - 1}{\rho^{2k} - 1}\right),$$

$$N_2 = -\frac{L}{B_{rr} - A_{rr}k}\left(\frac{\rho^{-k+1} - 1}{\rho^{-2k} - 1}\right),$$

$$P_1 = -\frac{M}{A_{rr}k + B_{rr}}\left(\frac{\rho^{k+1} - 1}{\rho^{2k} - 1}\right),$$

$$P_2 = -\frac{M}{B_{rr} - A_{rr}k}\left(\frac{\rho^{-k+1} - 1}{\rho^{-2k} - 1}\right),$$

and

$$L = \frac{D_{\theta\theta}(A_{rr} + B_{rr}) - D_{rr}(B_{rr} + B_{\theta\theta})}{A_{rr} - B_{\theta\theta}},$$

$$M = \frac{C_{rr}(B_{\theta\theta} + B_{rr}) - C_{\theta\theta}(A_{rr} + B_{rr})}{A_{rr} - B_{\theta\theta}}$$

Transverse deformation, ε_t, becomes

$$\begin{aligned}\varepsilon_t &= \varepsilon_{\theta\theta}\Big|_{r=R_1} = \frac{U_r}{r}\Big|_{r=R_1} \\ &= \left(N_1 \cdot \rho^{k-1} + N_2 \cdot \rho^{-k-1} + \frac{D_{\theta\theta} - D_{rr}}{A_{rr} - B_{\theta\theta}}\right)\varepsilon_{zz} \\ &\quad + \left(P_1 \cdot \rho^{k-1} + P_2 \cdot \rho^{-k-1} + \frac{C_{rr} - C_{\theta\theta}}{A_{rr} - B_{\theta\theta}}\right)\end{aligned} \tag{A2}$$

Appendix B: material tensors

$$A_{ij} = C^m_{ijrr} + C^f_{ijrr}, \quad B_{ij} = C^m_{ij\theta\theta} + C^f_{ij\theta\theta},$$

$$C_{ij} = C^m_{ijkl}\alpha^m_{kl} + \delta^f_{ij}, \quad D_{ij} = C^m_{ijzz} + C^f_{ijzz}$$

The expressions of C^m_{ijkl} and C^f_{ijkl} are given in Eqs. (4) and (8) (or Appendix C).

Appendix C: elastic properties of the microfibril skeleton

Where $c = \cos\varphi$ and $s = \sin\varphi$

$$C^f_{rrrr} = C^{f^*}_{1111} = 0$$

$$\begin{aligned}C^f_{\theta\theta\theta\theta} &= C^{f^*}_{2222}c^4 + 2\left(C^{f^*}_{2233} + 2C^{f^*}_{3232}\right)c^2s^2 + C^{f^*}_{3333}s^4 \\ &= E^f_3 s^2\left(s^2 + 4g \cdot c^2\right)\end{aligned}$$

$$\begin{aligned}C^f_{zzzz} &= C^{f^*}_{3333}c^4 + 2\left(C^{f^*}_{2233} + 2C^{f^*}_{3232}\right)c^2s^2 + C^{f^*}_{2222}s^4 \\ &= E^f_3 c^2\left(c^2 + 4g \cdot s^2\right)\end{aligned}$$

$$\begin{aligned}C^f_{z\theta z\theta} &= C^{f^*}_{3232}\left(c^2 - s^2\right)^2 + \left(C^{f^*}_{2222} + C^{f^*}_{3333} - 2C^{f^*}_{2233}\right)c^2s^2 \\ &= E^f_3\left[c^2s^2 + g \cdot \left(c^2 - s^2\right)^2\right]\end{aligned}$$

$$C^f_{rzrz} = C^{f^*}_{1313}c^2 + C^{f^*}_{1212}s^2 = g \cdot E^f_3 c^2,$$

$$C^f_{r\theta r\theta} = C^{f^*}_{1212}c^2 + C^{f^*}_{3131}s^2 = g \cdot E^f_3 s^2$$

$$C^f_{rr\theta\theta} = C^f_{\theta\theta rr} = C^{f^*}_{2211}c^2 + C^{f^*}_{3311}s^2 = 0$$

$$\begin{aligned}C^f_{\theta\theta zz} &= C^f_{zz\theta\theta} = C^{f^*}_{2233}\left(c^4 + s^4\right) \\ &\quad + \left(C^{f^*}_{2222} + C^{f^*}_{3333} - 4C^{f^*}_{3232}\right)c^2s^2 = E^f_3 c^2s^2(1 - 4g)\end{aligned}$$

$$C^f_{zzrr} = C^f_{rrzz} = C^{f^*}_{3311}c^2 + C^{f^*}_{2211}s^2 = 0$$